Decoration of Nickel and Magnesium Oxide Crystallites with Spinel-Type Phases

Bernadette Rebours, Jean-Baptiste d'Espinose de la Caillerie, and Olivier Clause*

Contribution from the Kinetics and Catalysis Division, Institut Français du Pétrole, BP 311, 92506 Rueil-Malmaison Cedex, France

Received March 19, 1993. Revised Manuscript Received August 28, 1993®

Abstract: The structure of the Al promoted magnesium and nickel oxides obtained by calcination of hydrotalcite-type coprecipitates was investigated by X-ray diffraction, ^{27}Al MAS–NMR, EXAFS, and alkaline leachings. In addition to the reflections of the MgO rock-salt type structure, the diffraction patterns of the Al modified MgO exhibited an additional, well-defined reflection at d = 0.253 nm, attributable to cations on tetrahedral sites. The tetrahedrally coordinated cations were likely to belong to a nonstoichiometric spinel-type phase including an excess of magnesium. The same behavior was observed when Ga(III) were substituted for Al(III) ions in the materials. Furthermore, in the Ga promoted magnesium oxides, EXAFS indicated that only a minor part of the Ga(III) ions was substitutionally dissolved in MgO. The nature of the phases present at the surface of the Al-modified magnesium and nickel oxides was investigated employing alkaline leachings with aqueous sodium hydroxide solutions on Al-doped NiO and with sodium ethoxide in anhydrous ethanol solutions on Al-doped MgO systems. In both cases, the selective dissolution of aluminum-rich phases at the surface of the mixed oxides was observed. ^{27}Al MAS–NMR before and after leachings confirmed that the surface of the Al modified MgO was enriched in tetrahedrally coordinated aluminum. The presence of an alumina phase at the surface of the Al promoted NiO was also suggested in view of the crystallization of boehmite upon hydrothermal treatments under moderate temperature and pressure, whereas more severe hydrothermal conditions led to hydrotalcite-like structure reconstitution. The aluminum distribution in the magnesium and nickel oxides is not homogeneous and the local composition of the mixed oxides fluctuates between magnesium (or nickel) and aluminum-rich phases. The Al-doped MgO or NiO particles can also be viewed as "decorated" by aluminate-type patches, which are thought to be responsible for their surface properties and for their resistance to sintering.

Introduction

Promotion of oxides with guest ions often results in valuable new effects such as modified surface electronic structures, enhanced reactivity, and improved catalytic properties. For example, modification with alkaline ions leads to a marked improvement of the MgO surface basicity and electron donating properties.[1-3] Also, the resistance to thermal sintering and phase transformation of many oxides can be controlled by textural promoters. The kinetics of phase separation in the TiO_2–SnO_2 solid solution is strongly influenced by the presence of dopants.[4,5]

The MgO–Al_2O_3 and NiO–Al_2O_3 mixed oxides obtained by calcination of hydrotalcite-type hydroxycarbonates constitute relevant examples of Al stabilized magnesium and nickel oxide phases. Promotion with Al^{3+} ions was reported to stabilize MgO toward sintering or crystallization, leading to potential application for stabilized magnesia as catalyst for aldol condensations, phthalic acid etherification, and propyleneoxide polymerization.[6] Owing to its improved stability toward heat and steam, the use of stabilized magnesia as novel support material was proposed.[7] Platinum and palladium clusters supported on Al stabilized MgO were found active and stable for hydrocarbon reforming reactions.[8-11] Al stabilized NiO systems are catalyst precursors for the steam reforming reaction and have received, for this reason, much attention in the last decades.[12,13]

The thermal decomposition of hydroxides and carbonates often produces very reactive oxides;[14-16] however, the reasons for the promoter effect of the aluminum ions are still a matter of debate. Concerning the Al-modified NiO system, various explanations for the thermal stability have been proposed. A two phase model comprising an Al-doped NiO phase and discrete nickel oxide particles was first suggested.[17] A different model consisting of the formation of a single, metastable Al-doped NiO phase upon calcination of hydrotalcite-type coprecipitates was later proposed.[18,19] This metastable phase was supposed to be the precursor to paracrystalline nickel particles after reduction, which accounted

* To whom correspondence should be addressed. Fax: 33 1 47 52 60 55.

® Abstract published in *Advance ACS Abstracts*, February 1, 1994.

(1) Klabunde, K. J.; Matsuhashi, H. *J. Am. Chem. Soc.* **1987**, *109*, 1111–1114.

(2) Zhang, G.; Tanaka, T.; Yamaguchi, T.; Hattori, H.; Tanabe, K. *J. Phys. Chem.* **1990**, *94*, 506–508.

(3) Driscoll, D. J.; Martir, W.; Wang, J.; Lunsford, J. H. *J. Am. Chem. Soc.* **1985**, *107*, 58–63. Ito, T. W.; Wang, J.; Lin, C.; Lunsford, J. H. *J. Am. Chem. Soc.* **1985**, *107*, 5062–5068. Lin, C.; Ito, T.; Wang, J.; Lunsford, J. H. *J. Am. Chem. Soc.* **1987**, *109*, 4808–4810.

(4) Virkar, A. V.; Plichta, M. R. *J. Am. Ceram. Soc.* **1983**, *66*, 451–456.

(5) Yuan, T. C.; Virkar, A. V. *J. Am. Ceram. Soc.* **1988**, *71*, 12–21.

(6) On the use of Al-promoted magnesium oxides for aldol condensation reactions, see, for example: Suzuki, E.; Ono, Y. *Bull. Chem. Soc. Jpn.* **1988**, *61*, 1008–1010. Reichle, W. T. *J. Catal.* **1985**, *94*, 547–557. Arena, B. J.; Holmgren, J. S. U.S. patent 5,144,089 to U.O.P. Corma, A.; Fornés, V.; Martin-Aranda, R. M.; Rey, F. *J. Catal.* **1992**, *134*, 58–65. On the use of MgO–Al_2O_3 mixed oxides for phthalic acid etherification, see: Nosawa, R. *Chem. Eng.* **1975**, *89*, 26–30. On the use of MgO–Al_2O_3 mixed oxides for propiolactone polymerization, see: Nakatsuka, T.; Kawasaki, H.; Yamashita, S.; Kohjiya, S. *Bull. Chem. Soc. Jpn.* **1979**, *52*, 2449–2450.

(7) Schaper, H.; Berg-Slot, J. J.; Stork, W. H. J. *Appl. Catal.* **1989**, *54*, 79–90.

(8) Davis, R. J.; Derouane, E. G. *Nature* **1991**, *349*, 313–315.

(9) Davis, R. J.; Derouane, E. G. *J. Catal.* **1991**, *132*, 269–274.

(10) Davis, R. J.; Derouane, E. G. *Proceedings of the 12th North American Meeting of the Catalysis Society*; Lexington; **1991**; C35.

(11) Davis, R. J.; Derouane, E. G. *Proceedings of the 10th International Congress Catalysis*; Budapest; **1992**; O68.

(12) Milligan, W. O.; Richardson, J. T. *J. Phys. Chem.* **1955**, *59*, 831–833.

(13) Rostrup-Nielsen, J. R. In *Steam Reforming Catalysts*; Teknisk Forlag: Copenhagen, 1975. Ross, J. R. H. In *Catalysis, Specialist Periodical Reports*; Royal Society of Chemistry: London, 1985; Vol. 7, pp 1–43.

(14) *Comprehensive Chemical Kinetics*; Bamford, C. H., Tipper, C. F. H., Eds; Elsevier: Amsterdam, 1980; Vol. 22, pp 241–246.

(15) Beruto, D.; Searcy, A. W. *Nature* **1976**, *263*, 221–222.

(16) Towe, K. M. *Nature* **1978**, *274*, 239–240.

(17) Alzamora, L.; Ross, J. R. H.; Kruissink, E. C.; Van Reijen, L. L. *J. Chem. Soc., Faraday Trans.* **1981**, *77*, 665–681.

(18) Puxley, D. C.; Kitchener, I. J.; Komodromos, C.; Parkyns, N. D. In *Preparation of Catalysts III*; Poncelet, G., Grange, P., Jacobs, P. A. Eds.; Elsevier: Amsterdam, 1983; pp 237–271.

(19) Wright, C. J.; Windsor, C. G.; Puxley, D. C. *J. Catal.* **1982**, *78*, 257–261.

0002-7863/94/1516-1707$04.50/0

for the high thermal stability of steam-reforming catalysts. Removal of nickel as nickel carbonyl, however, reveals a sponge-like alumina structure in the reduced catalysts.[20] The question arises as to whether alumina diffuses out of NiO during reduction and/or is already present in the calcined materials. Concerning the Al-modified MgO system, a model was proposed based on a previously published investigation on the structure of $ZnO–Cr_2O_3$ small particles.[21] Substitution of Mg(II) for Al(III) ions on octahedral sites in the MgO structure was suggested to lead to a surplus of O^{2-} surface ions, resulting in an energy stabilization of the system.[11] In another model, the presence of surface moieties $[Al_3Mg_6O_9]^{3+}$ was responsible for the increased Lewis acidity of the surface.[1]

Recently, the thermal decomposition of dolomite ($CaMg(CO_3)_2$) was suggested to lead to nonequilibrium oxide solutions whose formation was described along the lines of the theory of spinodal decompositions.[22,23] Compositional fluctuations from Mg to Ca rich regions with a spatial wavelength around 5 nm were observed. This study might constitute a guideline for the investigation of the thermal decomposition of hydrotalcite-like compounds. The surface compositions were, however, not investigated. As far as catalytic processes are involved, the characteristics of the surface of the Al modified magnesium and nickel oxides are of major importance. The oxide properties depend on whether or not their surface contain segregated dopants.[24]

The present paper concerns the bulk structure and surface composition of Al-modified magnesium and nickel oxides obtained by calcination of hydrotalcite-type coprecipitates. The magnesia-based systems have been carefully investigated by X-ray diffraction. The presence of a reflection normally absent in rock salt type structure patterns is reported and discussed. An analogous, additional reflection is also observed in Ga modified magnesium oxide obtained by calcination of Mg–Ga hydrotalcite. EXAFS is performed at the Ga K edge on the Ga promoted MgO. The surface composition of the mixed oxides is discussed in view of the results of alkaline leachings coupled with ^{27}Al MAS NMR experiments. A previous study on Al-doped nickel oxide showed that an aluminum-rich phase was removed by selective dissolution in concentrated aqueous sodium hydroxide solutions.[25] Such washing cannot be performed on the Al promoted MgO systems since these oxides readily rehydrate to reconstruct the hydrotalcite-type structure. Accordingly, anhydrous strongly basic solutions are used to avoid magnesia hydration. The selective removal of alumina and its effect on the mixed oxide thermal stability are discussed. Hydrothermal treatments under mild conditions are performed on the Al promoted nickel oxides and the presence of superficial alumina is confirmed. A model accounting for the surface enrichment in Al and for the thermal stability of the Al-modified NiO and MgO systems is proposed.

Experimental Section

The preparation of hydrotalcite-like materials $[Ni_{1-x}Al_x(OH)_2](CO_3)_{x/2}\cdot nH_2O$ ($0.25 < x < 0.33$) has been reported previously.[25,26]

Hydrotalcite-like materials $[Mg_{1-x}Al_x(OH)_2](CO_3)_{x/2}\cdot nH_2O$ (x = 0.35, 0.25, 0.15) and $[Mg_{1-x}Ga_x(OH)_2](CO_3)_{x/2}\cdot nH_2O$ ($x = 0.25$) were prepared at constant pH (equal to 9.0) and temperature (333 K). The precipitates were washed with distilled water until Na contents lower than 50 μg Na per g of sample were reached. The products were then dried for 16 h at 313 K and for 16 h at 373 K. The calcinations were performed in a muffle furnace during 16 h at temperatures ranging from 723 to 1423 K; the heating rates were 300 K/h. The magnesium based oxides were stored under anhydrous conditions. The amounts of Mg, Ni, Al, and Ga in the mixed oxides were determined by atomic absorption after acid extraction.

For the coprecipitates calcined at 923 K, N_2 adsorption–desorption isotherms were determined in a φsorb apparatus (GIRA) at 77 K following a pretreatment at 673 K under 10^{-4} Torr. The adsorption isotherms have been analyzed according to the Dubinin theory of pore volume filling and the B.E.T. theory. The Dubinin micropore volumes were extracted from the extrapolation to zero of the linear portion of the Dubinin plots.[27]

Alkaline leaching of the Ni–Al mixed oxides has been described elsewhere.[25] Sodium ethoxide was prepared by dissolving sodium metal with reaction in anhydrous ethanol. Freshly prepared sodium ethoxide solutions were used for basic leachings of the Mg–Al mixed oxides as follows: suspensions of 1 g of mixed oxides in 200 cm^3 of Na ethoxide solution were thoroughly stirred at 343 K for 4 h under argon. The containers were polyethylene-lined so as to avoid any glass dissolution and were shielded from light so as to minimize the formation of organic polymers. The suspensions were then centrifuged, and the resulting materials were rinsed with anhydrous ethanol. The solutions were evaporated in glass-free, polyethylene-lined containers at 353 K. The solid residues were dissolved in concentrated nitric acid, and the Al and Mg contents were determined by atomic absorption. The Mg and Al concentrations in the leached materials were also determined by atomic absorption after dissolution in aqueous nitric acid.

Details on the coupled thermogravimetric and mass spectrometry analysis and on X-ray powder diffraction pattern acquisitions were reported previously.[25] Model phase patterns and Fourier transform difference between calculated and experimental diagrams have been obtained using the Rietveld program package XRS82 developed by the Institut für Kristallographie und Petrographie (Dr. C. Baerlocher, Zürich, Switzerland). *In situ* XRD measurements were performed on a Siemens D5000 θ/θ diffractometer using an Anton Paar high-temperature cell and a position sensitive detector. Patterns were recorded at 873 K under flowing helium up to $2\theta = 60°$. Powdered samples were spread and heated on a platinum ribbon used as sample holder.

EXAFS measurements were performed at the LURE radiation synchrotron facility (Orsay, France) using the D44 X-ray beamline emitted by the DCI storage ring (positron energy: 1.85 GeV; ring current 300 mA). The spectra were recorded at ambient temperature in the transmission mode using two air filled ionization chambers. A channel-cut single crystal of silicon was used as the monochromator, the (331) reflection being used. The energies were scanned with 2 eV steps for EXAFS analysis. The resolution $\delta E/E$ at the Ni and Ga K-edges was 2×10^{-4}. EXAFS measurements were carried out five times for each sample. The samples were finely ground and homogeneously dispersed in cellulose pellets. The amounts of nickel or gallium in the pellets were calculated so that the absorption variations $\Delta(\mu x)$ through the edges ranged between 0.8 and 1.2. The absorptions μx beyond the Ni or Ga absorption edges never exceeded 2. The analysis of the EXAFS spectra was performed following standard procedures for background removal, extraction of the EXAFS signal, and normalization to the edge absorption. Fourier transforms were obtained after multiplication of the EXAFS signal by a factor k^3, using the same Hanning window for the references and the investigated systems.

The nuclear magnetic resonance (NMR) free induction decay (FID) measurements were performed on a Bruker MSL 400 instrument. The wide bore magnet was fitted with a high-speed magic angle spinning (MAS) Bruker probe. The samples were spun in 4-mm diameter rotors (ZrO_2). The acquisition time was 17.4 ms, and the number of accumulations were between 100 and 1000 depending on the intensity of the signal. All spectra were broadened by a 10-Hz exponential factor. At 9.4 T, the resonance frequency of ^{27}Al is 104.26 MHz. In order to assure quantitative measurements the following conditions were retained for the one-pulse experiments. The phase sequences included a 90°

(20) Doesburg, E. B. M.; Hakvoort, G.; Schaper, H.; van Reijen, L. L. *Appl. Catal.* **1983**, *7*, 85–90.
(21) Hojlund-Nielsen, P. E. *Nature* **1977**, *267*, 822–823.
(22) On the thermodynamics and kinetics of spinodal decomposition in metallic binary systems, see: Cahn, J. W. *J. Chem. Phys.* **1958**, *28*, 258–267. Cahn, J. W.; Hilliard, J. E. *J. Chem. Phys.* **1965**, *42*, 93–99.
(23) On the chemical decomposition of dolomite, see: Spinolo, G.; Anselmi-Tamburini, U. *Z. Naturforsch.* **1984**, *39a*, 975–980. Spinolo, G.; Anselmi-Tamburini, U. *Z. Naturforsch.* **1984**, *39a*, 981–985. Spinolo, G.; Anselmi-Tamburini, U. *J. Phys. Chem.* **1989**, *93*, 6837–6843.
(24) Dufour, L. C.; El Anssari, A. E.; Dufour, P.; Vareille, M. *Surf. Sci.* **1992**, *269/270*, 1173–1179.
(25) Clause, O.; Rebours, B.; Merlen, E.; Trifiro', F.; Vaccari, A. *J. Catal.* **1992**, *133*, 231–246.
(26) Clause, O.; Gazzano, M.; Trifiro', F.; Vaccari, A.; Zatorski, L. *Appl. Catal.* **1991**, *73*, 217–236.
(27) On the determination of micropore volume by the Dubinin theory, see: Gregg, S.J.; Sing, K. S. W. In *Adsorption, Surface Area and Porosity*; Academic Press: London, 1982.

Table 1. Chemical Composition and X-ray Diffraction Data for Samples A–E[a]

sample	chemical analysis Ni (wt%)	Mg (wt%)	Al (wt%)	Ga (wt%)	M(II)/M(III) molar ratio	sample formulas	hydrotalcite-like structure lattice constants (nm) *a*	*c*
A	39.7		7.3		2.5	$[Ni_{0.72}Al_{0.28}(OH)_2](CO_3)_{0.14}\cdot 0.54H_2O$	0.3035	2.293
B		19.5	11.6		1.8	$[Mg_{0.67}Al_{0.33}(OH)_2](CO_3)_{0.16}\cdot 0.30H_2O$	0.3047	2.283
C		23.4	8.6		3.0	$[Mg_{0.75}Al_{0.25}(OH)_2](CO_3)_{0.12}\cdot 0.61H_2O$	0.3060	2.323
D		25.7	5.9		4.8	$[Mg_{0.83}Al_{0.17}(OH)_2](CO_3)_{0.08}\cdot 0.70H_2O$	0.3085	2.379
E		20.6		19.3	3.0	$[Mg_{0.75}Ga_{0.25}(OH)_2](CO_3)_{0.02}(NO_3)_{0.21}\cdot 0.61H_2O$	0.3106	2.381

[a] Note: a blank indicates that the corresponding element is not present in the sample. The inaccuracy on the lattice parameters values is 5×10^{-4} nm for *a* and 2×10^{-3} nm for *c*.

quadratic phase detection, and the baseline was corrected by automatic zero filling of the free induction decay. The pulse length was limited to 0.6 μs; with such a narrow pulse ($<\pi/10$), only the central transition is excited and the spectra quantitatively reflects the relative populations. The recycle delay was 1 s; the absence of selective saturation was checked by increasing the delay 10-fold. The spinning speed was 10.0 kHz, and the chemical shifts referred to a 0.1 M $Al(NO_3)_3$ aqueous solution.

Results

Coprecipitate Characterization. Sample A was prepared by coprecipitation from nickel and aluminum nitrate salts at pH 8.1. Both Ni(II) and Al(III) ions quantitatively precipitated during preparation. The Ni and Al contents in sample A are reported in Table 1. The TG–DTG diagrams of sample A exhibited two weight losses at 490 and 630 K, due first to the loss of interlayer water and then to decarbonatation and dehydroxylation.[26,28–30] Samples B–E were prepared by coprecipitation at pH 9.0. Only carbonates were found to be present in the interlayers for samples B–D, whereas nitrates and carbonates were observed in sample E. In all samples, the dehydration and dehydroxylation were complete at 773 K. Carbonates and nitrates were quantitatively removed before 873 K. The sample formulas deduced from the H_2O, NO_2, and CO_2 weight losses are reported in Table 1.

XRD analysis revealed a well-crystallized hydrotalcite-like structure in all samples, see Figure 1. Hydrotalcite-type coprecipitates have a rhombohedral R-3m symmetry. The M(II) and M(III) cations are homogeneously arranged in brucite-type layers, the excess positive charge of the layers being compensated by carbonate or nitrate ions forming interlayers.[31] The *a* and *c* unit cell parameters extracted from the XRD data are reported in Table 1. The lattice parameter *a* is the distance between neighboring cations in the brucite-type layers. The parameter *c* is three times the distance between adjacent brucite-type layers. The parameter *a* increases with the ionic radii of the cations.[30] For example, samples C and E are magnesium based with the same Mg(II)/M(III) atomic ratio. Parameter *a* is significantly higher in sample E, see Table 1, which is related to the values of ionic radii $r_{Al^{3+}} = 0.050$ nm and $r_{Ga^{3+}} = 0.062$ nm.[32] In samples B–D, *c* increases with increasing M(II)/M(III) atomic ratio, see Table 1. The contraction of the basal spacing is hence directly related to the amount of carbonate ions in the interlayers, in accord with numerous studies.[28,30,31]

X-ray Diffraction Study of the Calcined MgAl Hydrotalcite-Type Coprecipitates. The X-ray diffraction patterns of sample C calcined at temperatures ranging from 393 to 1423 K are shown in Figure 2. The observed phase transformations are in agreement with the literature.[30,33–36] The hydrotalcite reflections are observed for calcination temperatures up to 623 K. The XRD pattern of poorly crystallized MgO is observed from 623 to 1073 K, whereas a phase separation between MgO and the spinel $MgAl_2O_4$ occurs for calcination temperatures higher than 1073 K. Demixing is complete for calcination temperatures higher than 1423 K. This thermal behavior is independent of the Mg/Al ratio and is also observed when aluminum is replaced by gallium (sample E). In the latter case, however, demixing in pure magnesium oxide and magnesium gallate phases occurs at lower temperature, i.e., approximately 923 K.

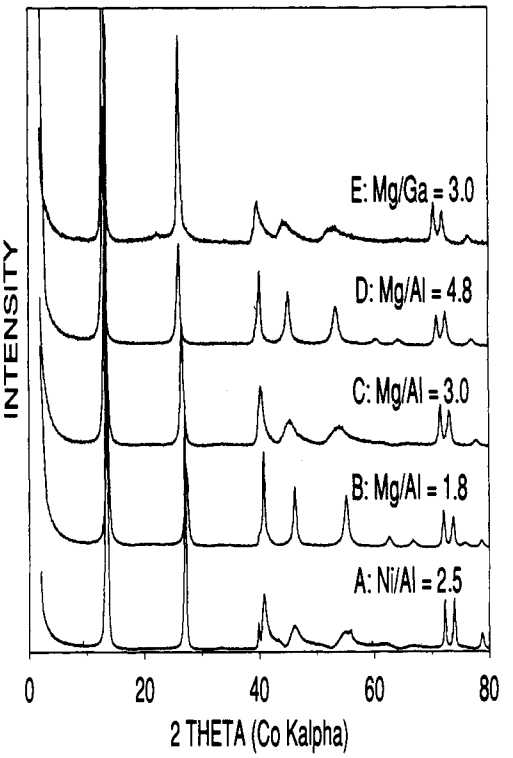

Figure 1. XRD powder patterns of samples A–E dried at 373 K.

Samples calcined in the 723–923 K range are poorly crystallized: it must be stressed that in addition to the MgO phase, amorphous phases can be present and even preponderant.[37,38] The pattern of sample C calcined between 673 and 1223 K reveals a broad reflection at approximately $d = 0.253$ nm ($2\Theta = 41.4°$, 2Θ refering to the Co Kα radiation) which does not belong to the MgO structure and overlaps the (111) reflection, see Figure 2. This reflection is also observed in the patterns of calcined samples B and D, see Figure 3, and disappears after complete demixing into magnesium oxide and spinel. Furthermore, a similar

(28) Kruissink, E. C.; van Reijen, L. L.; Ross, J. R. H. *J. Chem. Soc., Faraday Trans.* **1981**, *77*, 649–663.
(29) Hernandez, M. J.; Ulibarri, M. A.; Rendon, J. L.; Serna, C. J. *Thermochim. Acta* **1984**, *81*, 311–318.
(30) Sato, T.; Fujita, H.; Endo, T.; Shimada, M.; Tsunashima, A. *React. Solids* **1988**, *5*, 219–228.
(31) Cavani, F.; Trifiro', F.; Vaccari, A. *Catal. Today* **1991**, *11*, 173–302.
(32) Pauling, L. In *The Nature of the Chemical Bond*; Cornell University Press: New York, 1960.
(33) Miyata, S.; Okada, A. *Clays Clay Miner.* **1977**, *25*, 14–18.
(34) Reichle, W. T.; Kang, S. Y.; Everhardt, D. S. *J. Catal.* **1986**, *101*, 352–359.
(35) Sato, T.; Wakabayashi, T.; Shimada, M. *Ind. Eng. Chem. Prod. Res. Dev.* **1986**, *25*, 89–92.
(36) Rey, F.; Fornes, V.; Rojo, J. M. *J. Chem. Soc., Faraday Trans.* **1992**, *88*, 2233–2238.
(37) Szymanski, R.; Travers, C.; Chaumette, P.; Courty, P.; Durand, D. In *Preparation of Catalysts IV*; Delmon, B., Grange, P., Jacobs, P. A., Poncelet, G., Eds.; Elsevier: Amsterdam, 1987; pp 739–751.
(38) Thevenot, F.; Szymanski, R.; Chaumette, P. *Clays Clay Miner.* **1989**, *37*, 396–402.

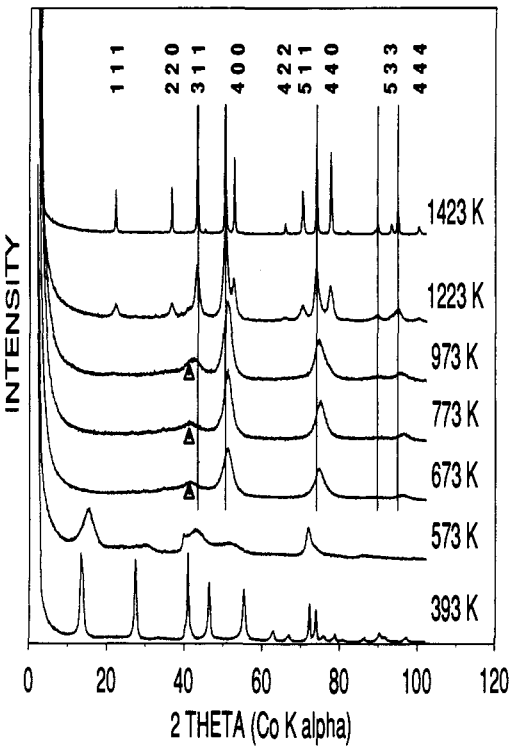

Figure 2. XRD powder patterns of sample B calcined from 393 to 1423 K. Values given above the peaks are magnesium aluminate *hkl*'s with their position in pure $MgAl_2O_4$. The reflections of pure MgO (cubic cell) are indicated by lines.

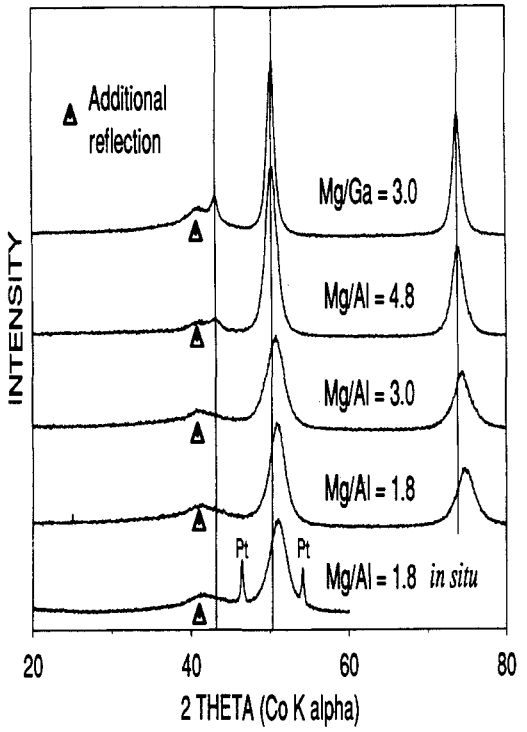

Figure 3. XRD powder patterns of samples B–E calcined at 873 K recorded in air along with the XRD pattern of sample B calcined *in situ* at 873 K under dry atmosphere. The reflections of pure magnesia (cubic cell) are indicated by lines and the additional reflection by a triangle.

additional reflection at $d = 0.256$ nm ($2\Theta = 40.9°$) is observed in the Ga-modified MgO obtained by calcination of sample E, see Figure 3. In the latter case, the (111) reflection is more intense and hence can be clearly distinguished from the additional reflection.

The additional reflection is not due to a partial rehydration of the mixed oxides. Indeed, XRD profiles were also recorded using an *in situ* cell allowing heating of samples under controlled dry atmosphere, see Figure 3. The observed platinum reflections are due to the platinum ribbon (sample holder) underneath the sample. Patterns similar to those recorded in air without the cell were obtained.

The reflection at $d = 0.253$ nm may arise from the presence of magnesium aluminate in addition to MgO. Indeed, the additional reflection can be attributed to the spinel most intense reflection (311) shifted toward lower 2Θ values, see Figure 2. The spinel lattice parameter (cubic cell) is estimated to be roughly 0.839 nm instead of 0.808 nm in pure stoichiometric magnesium aluminate. The difference can be due to a magnesium excess in the spinel-type structure. It is interesting to note that the spinel lattice parameter is twice the lattice parameter of the MgO phase calculated from the (111), (200), and (220) reflections, i.e., 0.419 nm. Thus, there is a strong correlation, likely an epitaxy, between the magnesium aluminate and the magnesia lattices.

This observation suggests that the observed reflections, including the additional reflection, might be due to a single phase, through the formation of a superstructure or the location of cations on tetrahedral sites inside the MgO lattice. In the former case, the aluminum ions substitute for Mg(II) ions on octahedral sites, and the cationic vacancies arrange themselves in an orderly way, so as to give new reflections. In the latter, a fraction of cations migrates from octahedral to tetrahedral sites which should lead to a modification of the XRD patterns. Both hypothesis were successively examined. For this purpose, we calculated ideal XRD powder patterns for calcined sample B. Obviously, in view of the low number of reflections available and the extensive reflection overlap in the XRD profiles, no attempt was made to refine the observed patterns. Nevertheless, Rietveld programs were used to attain more information on cation location and on the reflection at $d = 0.253$ nm.

First Model (Model 1): Al(III) Substituted for Mg(II) Ions in the MgO Lattice. The magnesium and aluminum cations were first constrained to remain on octahedral sites. Since isoelectronic Mg(II) and Al(III) ions have very close scattering factors, they were considered as undistinguishable, which is more than justified in view of the bad crystallinity of calcined sample B. A magnesia cell of $a = 0.839$ nm in space group $Fd3m$, made up with 32 oxygen anions and 32 magnesium cations, was used in these calculations. The oxygen sites were kept fully occupied, and the FWHM were kept constant. Among the 32 octahedral sites in the MgO lattice, the 16 octahedral sites which would be filled in the ideal spinel lattice were defined as octahedral(1), and the 16 octahedral sites vacant in the spinel lattice as octahedral(2). The site occupancies in perfect MgO and $MgAl_2O_4$ lattices are indicated in Table 2.[39] The cationic site occupancies refer to Mg or Al cations.

Cation vacancies were introduced to maintain electrical neutrality of the structure. Only the location of vacancies was allowed to vary. The best fit is shown in Figure 4 and the corresponding site occupancies are reported in Table 2, see model 1. It can be seen that, even though an adequate ordering of the cation vacancies induces a new reflection at $d = 0.253$ nm, the agreement with the observed profile is poor. It can also be observed that in the best fit vacancies are confined to octahedral(2) sites, i.e., to sites which are also vacant in the spinel structure.

Improved Model (Model 2): Cations on Interstitial Position. The difference Fourier map between the experimental and model 1 profiles is shown in Figure 5. The fourier transform intensity is indicated in the plane $z = 0$ along with the positions of cations and oxygen anions in the planes $z \pm 0.125$. The maximum intensity is located near the origin and equivalent positions, i.e., the location of tetrahedral sites in the spinel structure. Missing cations on tetrahedral sites are clearly revealed.

(39) On the structure and atomic parameters of the $MgAl_2O_4$ spinel in the space group $Fd3m$, see, for example: Ishii, M., Hiraishi, J.; Yamanaka Y. *Phys. Chem. Miner.* **1982**, *8*, 64–68.

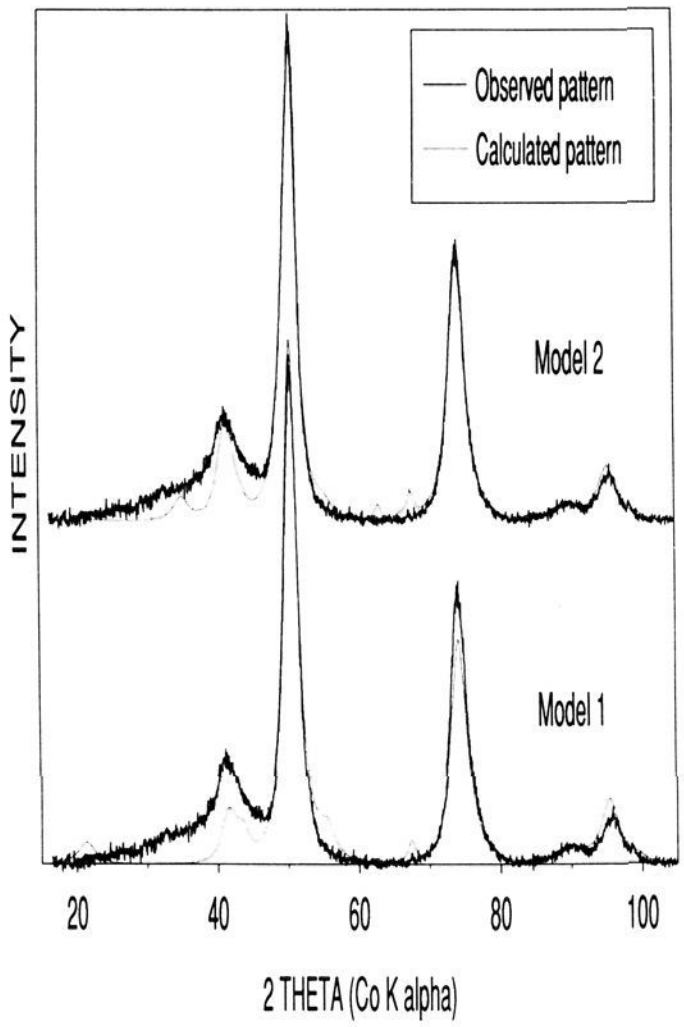

Figure 4. Top: XRD powder pattern of sample B calcined at 923 K (full line) along with the calculated pattern of model 2 (dotted line). Bottom: XRD powder pattern of sample B calcined at 923 K (full line) along with the calculated pattern of model 1 (dotted line).

Table 2. Site Occupancies for MgO, $MgAl_2O_4$, and Models

site	$x = y = z$	Wyckoff positions	MgO	$MgAl_2O_4$[39]	model 1	model 2
oxygen	0.365	32e	1	1	1	1
octahedral (1)	0.125	16c	1	1	1.17	1.0
octahedral (2)	0.625	16d	1	0	0.58	0.53
tetrahedral	0.250	8a	0	1	0	0.42

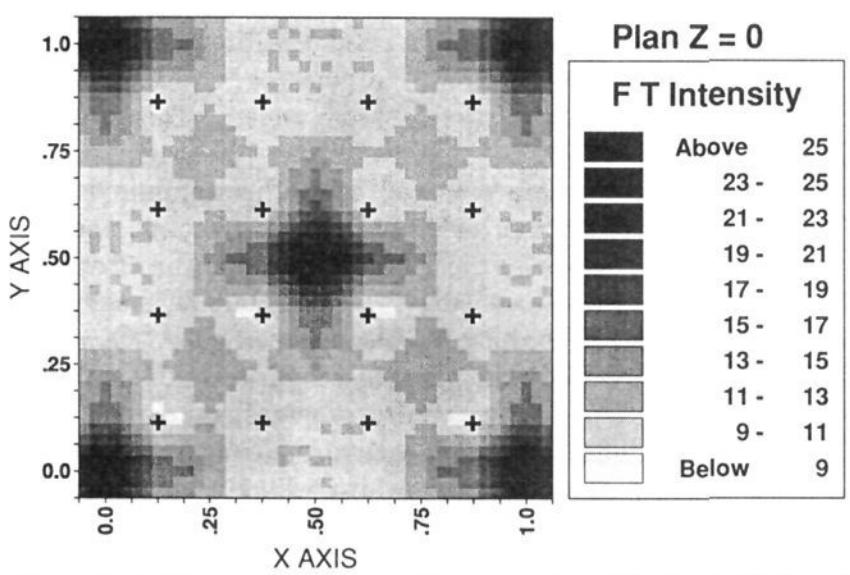

Figure 5. Difference fourier map for sample B calcined at 923 K and model 1.

The model was updated by incorporating cations on tetrahedral, interstitial sites. The best fit is shown in Figure 4. It can be seen that the calculated and observed reflection intensities are in better agreement than for model 1, even though the fit is not perfect. The fraction of tetrahedrally coordinated cations is found to be 0.114, see model 2 in Table 2. The width of the calculated additional reflection is lower than the observed width. Since the starting coprecipitates have only octahedral ions, this may reflect the disorder induced by diffusion of cations from octahedral to tetrahedral sites. On the other hand, the visible difference between the widths of the additional and of the magnesia reflections may reflect the presence of two different phases, i.e., a spinel-type phase in addition to MgO, the former being more disordered than the latter.

XRD profile calculations were also performed on calcined sample E ($MgO–Ga_2O_3$ mixed oxide). The Mg and Ga cations were first constrained to remain on octahedral sites and the location of cationic vacancies was allowed to vary. The relative intensities of the experimental reflections were not matched correctly. In a further model, cations were allowed to occupy tetrahedral sites. We found that the location of approximately one-third of Ga(III) cations on tetrahedral sites was required to fit the observed profile. Thus, as in the case of the $MgO–Al_2O_3$ system, the additional reflection can be attributed either to the presence of a phase such as magnesium gallate in addition to MgO, or to the presence of cations, likely Ga ions, on tetrahedral sites in the magnesia lattice.

In brief, the following conclusions can be drawn: (1) the XRD profiles of the mixed oxides obtained after calcining MgAl hydrotalcites between 723 and 923 K exhibit reflections characteristic of an Al-doped MgO phase plus an additional reflection at $d = 0.253$ nm which does not belong to the MgO structure. (2) the additional reflection is attributed to the presence of cations on tetrahedral sites. The tetrahedrally coordinated cations may belong to a nonstoichiometric magnesium aluminate-type phase including an excess of magnesium in addition to the Al-doped MgO phase. The magnesium excess as well as the presence of cations on tetrahedral sites accounts for a larger disorder in the spinel-type structure. Nevertheless, the 4-fold coordinated cations may also be included inside the MgO lattice, see model 2. (3) the same conclusions are valid when Ga^{3+} ions are substituted for Al^{3+} ions in the mixed oxides.

EXAFS Study of the $MgO–Ga_2O_3$ Mixed Oxides at the Ga K-Edge. In the preceding section we have suggested that part of the Ga^{3+} ions were located on tetrahedral sites, inside the MgO crystallites, or in a separate phase. In this section we show that the EXAFS technique can provide additional qualitative information on this system.

The Fourier-transformed EXAFS spectrum at the Ga K-edge of sample E dried at 373 K and sample E calcined at 873 K are shown in Figure 6. Fourier transforms were performed over a 4.0–12.5 $Å^{-1}$ range after multiplication by a k^3 factor. Dried sample E can be considered as a convenient reference compound for the Ga(III)–O absorber-backscatterer pair. Indeed, the structure of the cationic layers is the same in hydrotalcite-like sample E and $Mg(OH)_2$. The nearest backscatterers about the Ga(III) ions in sample E are six oxygen atoms belonging to OH groups. Furthermore, the lattice parameter a for sample E and magnesium hydroxide are very similar, i.e., 0.3106 nm for sample E and 0.3114 nm for $Mg(OH)_2$.[40] Thus, the Mg–OH and Ga–OH distances in sample E are likely to be very close to the Mg–OH distance in $Mg(OH)_2$, i.e., 0.210 nm.[40] Moreover, the next nearest Mg + Ga shell is located far beyond the oxygen shell (around 3.2 Å).

The analysis of the nearest neighbor peak in sample E calcined at 823 K was performed after Fourier backtransform over a 1.11–1.73 Å range using phase shift and backscattering amplitude functions extracted from dried sample E data. An excellent fit was obtained with 4.5 ± 1.0 oxygen backscatterers at 1.98 ± 0.03 Å around the Ga(III) ions ($\Delta\sigma^2 = 0.0044$ Å^2). The Ga–O distance is intermediate to those reported for gallium(III) in tetrahedral and in octahedral coordination, i.e., 1.80–1.83 Å for tetrahedrally coordinated gallium(III) in the β-Ga_2O_3 structure and 1.99–2.02 Å for octahedrally coordinated gallium in the α and β-Ga_2O_3

(40) See: *Gmelins Handbuch der Anorganischen Chemie*; Vol. 27; Verlag Chemie: Weinheim, 1937; p 27.

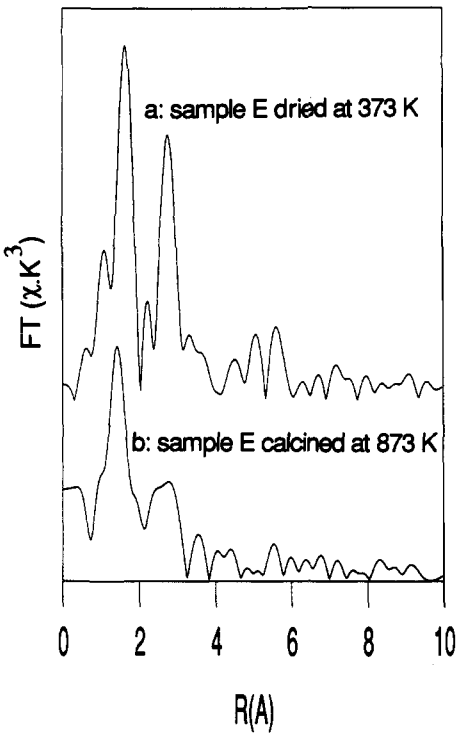

Figure 6. (a) Fourier transformed EXAFS spectrum (k^3 weighted; without phase correction) at the Ga K edge of sample E dried at 373 K. (b) Fourier transformed EXAFS spectrum (k^3 weighted; without phase correction) at the Ga K edge of sample E calcined at 873 K.

structures.[41] The coordination number is significantly lower than 6, indicating that part of the gallium cations is tetrahedrally coordinated. Finally, the existence of two slightly different but unresolved Ga–O distances, or an increase of structure disorder induced by heating, may account for the large increase of the differential Debye–Waller factor $\Delta\sigma^2$.

The most relevant information is given by the qualitative examination of the next nearest backscatterer peaks. In dried sample E, the Mg^{2+} and Ga^{3+} ions are homogeneously arranged in brucite-type, octahedral layers (hydrotalcite-like structure). Thus the next nearest backscatterers around the gallium ions are six magnesium or gallium cations located at 0.3106 nm, see Table 1. They produce an intense peak around 3 Å in the Fourier-transformed spectrum at the Ga K-edge, see Figure 6a. This intense peak along with the double peak between 5 and 6 Å is characteristic of hydrotalcite-like structures. These features are present in the Fourier transformed EXAFS spectra of a large number of mixed hydroxides, such as cobalt–aluminum, nickel–aluminum, and zinc–aluminum coprecipitates.[25,42] We observe that the interferences between electronic waves scattered by Mg and Ga atoms located at the same distances about the Ga^{3+} ions are not destructive. This information is useful to interpret the low intensity of the next nearest backscatterer peak in the Fourier-transformed EXAFS spectrum of calcined sample E, see Figure 6b. The MgO crystallite size deduced from XRD line broadening is approximately 6 nm in calcined sample E. In a previous study, we observed that the contribution of Ni(II) surface ions in NiO crystallites having a size of 5.5 nm was negligible in comparison with that of bulk ions.[25] In other words, NiO or MgO crystallites having a size higher than 6 nm cannot be distinguished from bulk oxides by EXAFS. Thus, the weakness of the peaks observed between 2 and 3 Å in Figure 6b is not attributable to a bulk/surface ratio effect. Now, if significant amounts of Ga^{3+} ions were substituted for Mg^{2+} ions in the MgO crystallites, the next nearest coordination shell in the MgO rock-salt-type structure should contain nine Mg and three Ga atoms located at approximately 2.98 Å. This contribution should give rise to an intense peak at about 3 Å in Figure 6b, two times more intense than that observed in Figure 6a. Without attempting to specify the nature of backscatterers responsible for the small peaks between 2 and 3 Å in Figure 6b, we can conclude that only a minor part of the Ga^{3+} ions are substitutionally dissolved in the MgO lattice. The greater part of gallium ions are either inserted on tetrahedral sites in MgO or forming another phase, possibly magnesium gallate or gallium oxide.

In short, the EXAFS study indicates that the gallium ions are both on octahedral and tetrahedral sites. Furthermore, only a minor part of gallium substitutes for magnesium in the magnesia lattice. Thus, the presence of gallium-rich phase(s) in addition to MgO is highly probable.

Table 3. Textural Properties of Samples A–D Calcined at 923 K

sample	surface area ($m^2\ g^{-1}$)	pore volume ($cm^3\ g^{-1}$)	micropore (Dubinin) vol ($cm^3\ g^{-1}$)
A	152	0.31	0.062
B	198	0.35	0.089
C	208	0.30	0.084
D	161	0.30	0.076
E	86	0.20	0.035

Textural Properties of Samples A–E Calcined at 923 K. Specific surface area and pore volume measurements are gathered in Table 3. The surface area decreases with increasing weight of the metal components. The N_2 adsorption-desorption isotherms for samples A–E are very similar to those typically observed with γ-alumina samples. The micropore volumes (radii < 2 nm) as determined by the Dubinin method are small and constitute from 15 to 20% of the total pore volumes. Thus, calcined samples A–E cannot be considered as microporous systems, such as zeolites for example, even though the greater part of the observed surface areas originates from the micropore volumes.

Effect of Hydrothermal Treatments on the NiO–Al_2O_3 Mixed Oxides. The NiO–Al_2O_3 and MgO–Al_2O_3 mixed oxides obtained by calcination of hydrotalcite-type coprecipitates at temperatures lower than required for the spinel crystallization are known to reconstruct under hydrothermal treatments, i.e., to revert back to the original structure of the coprecipitates.[43] This effect is sometimes referred to as a "memory" effect. For significantly higher calcination temperatures, well crystallized aluminate and NiO or MgO phases are revealed by X-ray diffraction and the memory effect, as well as the thermal stability of the mixed oxides, are lost. The ability to reconstruct the hydrotalcite structure is somewhat different for the NiO–Al_2O_3 and the MgO–Al_2O_3 mixed oxides. The MgO based oxides readily rehydrate under ambient temperature and atmospheric pressure: whereas, severe conditions are required to reconstitute the Ni–Al hydrotalcite-like structures. As previously reported in the literature, we have observed that the Ni–Al hydrotalcite structures were reconstructed upon energetic stirring of aqueous suspensions of the NiO–Al_2O_3 mixed oxides at 523 K, under 4 MPa, during 12 h.[30]

Keeping in mind that the studied mixed oxides are not microporous, we attempted to selectively rehydrate the surface region of the Al-doped NiO crystallites by performing hydrothermal treatments under moderate temperature (473 K) and pressure (2 MPa) on sample A calcined at 923 K. The X-ray diffraction patterns of sample A calcined at 923 K, sample A calcined at 923 K and then submitted to a hydrothermal treatment during 2 h, and sample A calcined at 923 K and then submitted to a hydrothermal treatment during 12 h are shown in Figure 7. The following is observed: (1) The mixed oxides are not fully

(41) Geller, S. *J. Chem. Phys.* **1960**, *33*, 676–684. Cotton, F. A.; Wilkinson, G. In *Advanced Inorganic Chemistry*; Wiley: New York, 1988; p 212. *Gmelins Handbuch der Anorganischen Chemie*; Verlag Chemie: Weinheim, 1937; Vol. 36; p 68.

(42) Paulhiac, J. L., Clause, O. *J. Am. Chem. Soc.* **1993**, *115*, 11602–11603.

(43) Courty, Ph.; Marcilly, C. In *Preparation of Catalysts III*; Poncelet, G., Grange, P., Jacobs, P. A. Eds.; Elsevier: Amsterdam, 1983; pp 485–517.

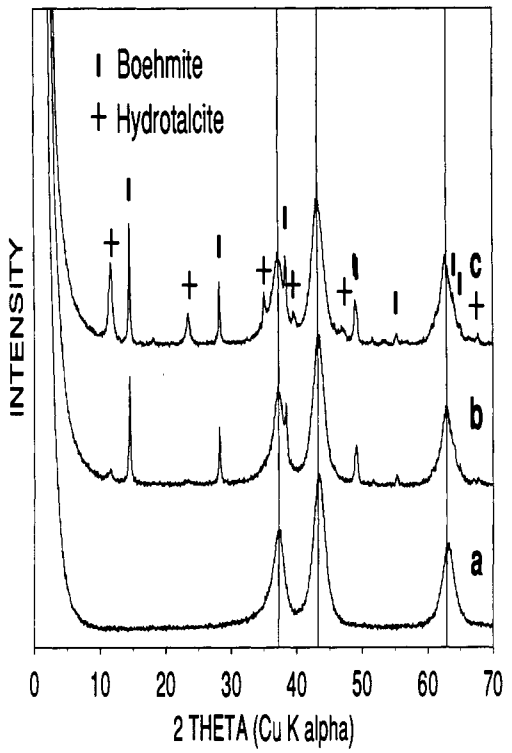

Figure 7. XRD powder patterns of sample A calcined at 923 K (a), sample A calcined at 923 K then submitted (b) to an hydrothermal treatment during 2 h, and (c) to an hydrothermal treatment during 12 h.

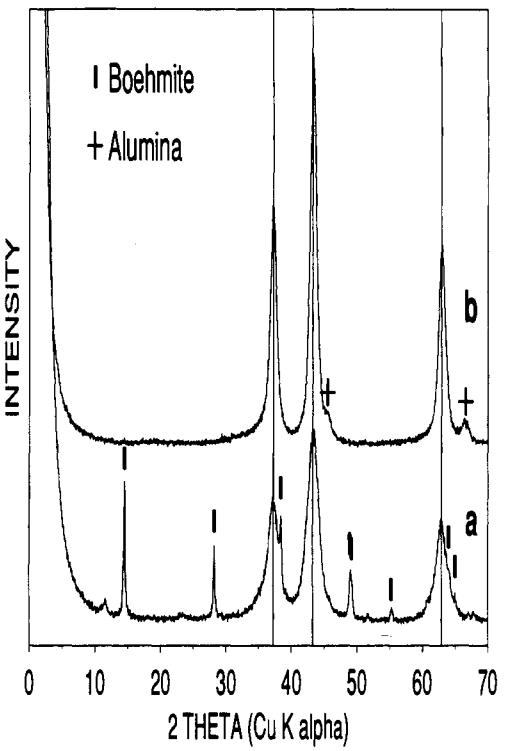

Figure 8. XRD powder patterns of sample A calcined at 923 K after hydrothermal treatment during 2 h (a) and of the same sample recalcined at 923 K after hydrothermal treatment (b).

rehydrated. NiO particles are observed with the same lattice parameters and average crystal size as before treatment. (2) A well-crystallized, boehmite phase is formed initially. The positions and relative intensities of the reflections are close to those of pure, undoped boehmite. After approximately a 2-h hydrothermal treatment, the amount of formed boehmite reaches a plateau; no nickel hydroxide formation is revealed, only a weak reflection attributed to an hydrotalcite-type phase starts to appear. (3) A hydrotalcite-like phase is formed subsequently to boehmite crystallization.

The XRD pattern of sample A calcined at 923 K, then hydrothermally treated as described above during 2 h, and the pattern of the same sample after subsequent calcination at 923 K for 16 h are shown in Figure 8. Alumina, possibly γ-Al_2O_3, is visible in the profile of the calcined sample. The NiO average crystal size slightly increases upon calcination.

Effect of Alkaline Leachings on the NiO–Al_2O_3 and MgO–Al_2O_3 Mixed Oxides. In order to separate nickel or magnesium oxide from aluminum-rich phases by selective dissolution, leaching of the NiO–Al_2O_3 and MgO–Al_2O_3 mixed oxides with acidic and alkaline solutions was performed. All samples were found to be completely soluble in acidic solutions. Leaching with aqueous or organic alkaline solutions, however, removed significant amounts of aluminum ions by dissolution into the liquid phase. We successively focused on alkaline leachings performed on NiO and then on MgO based mixed oxides.

Preliminary washing experiments of the NiO–Al_2O_3 mixed oxides with concentrated aqueous sodium hydroxide solutions have been previously reported.[25] We observed that the Al(III) concentrations in the NaOH solutions attained a plateau after 2 h of leaching at 363 K. The quantity of Al(III) ions remaining in the leached mixed oxides was independent of the volume of the NaOH solution. Approximately two-thirds of the aluminum initially present in the mixed oxides was removed, see Table 4. By contrast, the Ni(II) concentration in the leaching solutions was always very low, which was attributed to the low solubility of nickel hydroxide at pH 14. The precipitation of nickel hydroxide onto the mixed oxides during the NaOH leaching was not excluded. It is of major importance, in order to draw firm conclusions about the composition of the phase which dissolves during leaching, to estimate the amount of deposited $Ni(OH)_2$, and then to compare it with the amount of dissolved Al(III) ions.

We have studied the effect of alkaline leaching on sample A calcined at 1023 K by EXAFS spectroscopy at the Ni K-edge. The experimental procedure for leaching was described previously.[25] Approximately 60% of aluminum initially present in calcined sample A is removed. The Fourier transformed EXAFS spectra of sample A calcined at 1023 K before and after NaOH leaching are shown in Figure 9. The first peak from the origin is due to six oxygen backscatterers about the octahedrally coordinated Ni(II) ions.[25] The peak located between 2 and 3 Å in Figure 10 is due to 12 nickel- or aluminum-type next nearest backscatterers.[25] The six next nearest Ni(II) cations around the Ni atoms in $Ni(OH)_2$ produce a less intense peak in the Fourier tranformed EXAFS spectrum, which may be compared with that observed for sample E in Figure 6a.[44] Thus, if significant amounts of Ni(II) ions formed nickel hydroxide after leaching, a significant decrease of the height of the next nearest neighbor peak should be observed. On the contrary, the spectra before and after leaching are undistinguishable, see Figure 10, even though two-thirds of aluminum initially present in sample A have been removed. The amount of nickel hydroxide formed during leaching is hence very low. The phase which passes into solution is actually an aluminum-rich phase, likely a Ni-doped alumina.

It was also tempting to perform alkaline leaching on the MgO–Al_2O_3 mixed oxides. Unfortunately, aqueous sodium hydroxide solutions could not be used since the MgO based oxides readily rehydrated. Aluminum removal and rehydration occurred simultaneously so that firm conclusions could not be drawn. To avoid hydroxide reconstitution, we performed leaching experiments with anhydrous solutions of sodium ethoxide in ethanol,

(44) Clause, O.; Kermarec, M.; Bonneviot, L.; Villain, F.; Che, M. *J. Am. Chem. Soc.* **1992**, *114*, 4709–4717.

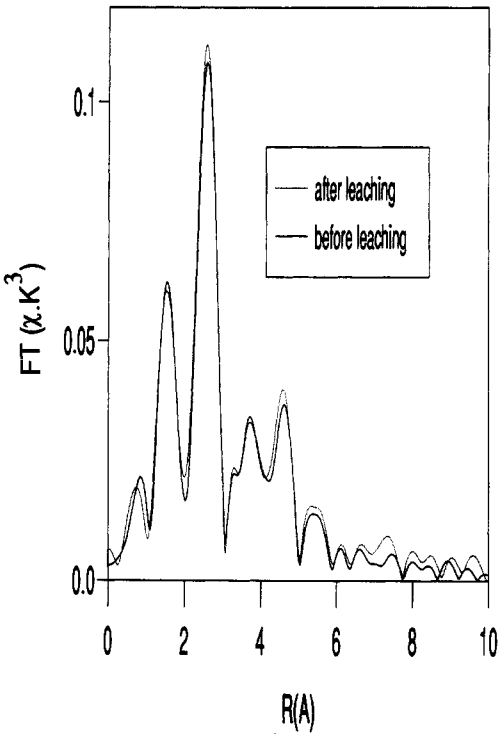

Figure 9. Fourier transformed EXAFS spectrum (k^3 weighted; without phase correction) at the Ni K edge of sample A calcined at 1023 K before and after alkaline leaching.

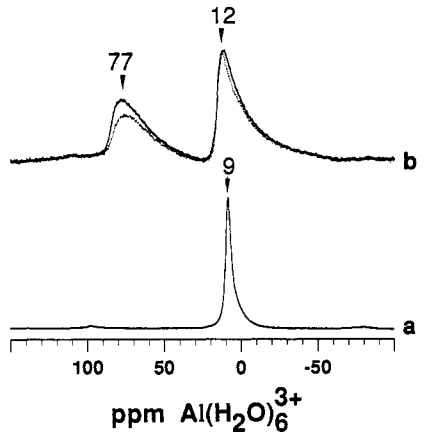

Figure 10. ^{27}Al MAS–NMR spectra of (a) sample D and (b) sample D calcined at 873 K before (full line) and after (dotted line) alkaline leaching.

whose basic properties are well known in organic chemistry.[45] Alkaline leaching was performed on samples B–D calcined at 923 K, see Table 4. The amount of aluminum passing into solution was found to reach a plateau after 4 h leaching at 434 K and was independent of the volume of alkaline solution used. The Mg/Al ratio measured directly in the leached oxides was in good agreement with that deduced from the aluminum passed into solution. Around one-third of Al(III) ions initially present in the mixed oxides was removed, compared to two thirds for the case of NiO-based oxides. The amount of magnesium ions which passed into solution was always extremely low.

Evolution of the aluminum coordination in sample D upon calcination and alkaline leaching was investigated by ^{27}Al MAS–NMR, see Figure 10. The hydrotalcite precursor spectrum reveals only one sharp asymmetric line with a maximum at 9 ppm, see Figure 10a. Upon calcination at 873 K the signal is considerably broadened, and the number of acquisitions had to be increased 10-fold to obtain a comparable signal-to-noise ratio. Two highly

(45) Cotton, F. A.; Wilkinson, G. In *Advanced Inorganic Chemistry*; Wiley: New York, 1988, p 127.

Table 4. Alkaline Leachings on Samples A–D Calcined at 923 K: Effect of Leaching Time

sample	leaching time (h)	metal concentrations in the leaching solutions (mg/L) Al(III)	Ni or Mg(II)	Al fraction removed[a] (at %)
A	5	145[b]	<0.2	64
B	1	120[c]	<0.5	17
	4	205[c]	1.6	29
	7	211[c]	4.5	30
C	4	140[c]	<0.5	25
D	4	150[c]	<0.5	30

[a] With respect to the total aluminum content of sample. [b] Leaching of 0.2 g of sample in 100 cm³ of solution. [c] Leaching of 1 g of sample in 200 cm³ of solution.

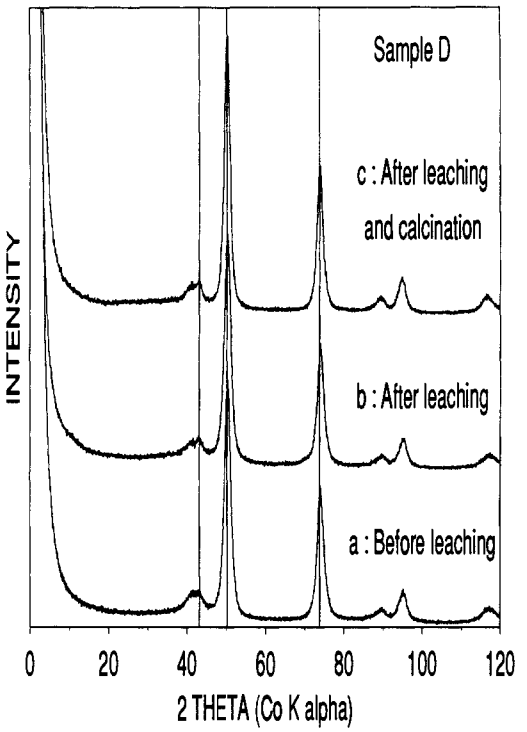

Figure 11. XRD powder patterns of sample D calcined at 923 K (a), sample D calcined at 923 K after leaching (b), and sample D calcined at 923 K after leaching and calcination (c).

asymmetrical lines attributable to 4- and 6-fold coordinated Al are resolved with maxima at 77 and 12 ppm respectively, see Figure 10b.[46] Careful phasing of the spectra leading to reproducible baseline and meaningful relative quantification gives $Al^{IV}/Al^{VI} = 0.70 \pm 0.03$.[47] After alkaline leaching, the line at 77 ppm has visibly diminished, and the Al^{IV}/Al^{VI} ratio is now 0.59 ± 0.03.

The XRD patterns of sample D calcined at 923 K before and after leaching is shown in Figure 11 along with the pattern of sample D calcined at 923 K after leaching. Leaching has no visible effect. In particular, the reflection attributed either to a spinel-type phase or to the tetrahedrally coordinated ion sublattice is not modified. Calcination results in a slight decrease of the width of the MgO reflections, i.e., a slight increase of the MgO average crystal size or a lower disorder in the MgO structure. Nevertheless, leaching does not alter substantially the thermal stability of the system.

(46) Lippmaa, E.; Samoson, A.; Mägi, M. *J. Am. Chem. Soc* **1986**, *108*, 1730–1735.

(47) For a thorough discussion on the reliability of ^{27}Al MAS–NMR quantifications, see, for example: Morris, H. D.; Bank, S.; Ellis, P. D. *J. Phys. Chem.* **1990**, *94*, 3121–3129, and references therein. Taulelle, F.; Bessada, C.; Massiot, D. *J. Chim. Phys.* **1992**, *89*, 379–385.

Discussion

Characterization of the Mixed Oxides by X-ray Diffraction and EXAFS. Numerous studies devoted to the hydrotalcite-type mixed hydroxides have concluded that the cations were homogeneously arranged in the coprecipitates.[18,25,30] The EXAFS, TGA, and ^{27}Al MAS–NMR techniques were shown to be useful to ensure that no separation of discrete aluminum or nickel hydroxide phases occurred during preparation of sample A.[25,48] The ^{27}Al MAS–NMR spectrum of sample D before calcination reveals a single sharp line attributable to Al^{VI}, which is consistent with the assumption of a single phase product, see Figure 10. The homogeneous distribution of cations in the oxide precursors is generally thought to be at the root of the thermal stability of the calcined materials. The aluminum distribution in the mixed oxides, however, has been less thoroughly investigated partly due to the poor crystallinity of the materials. Indeed, the XRD patterns of calcined Ni–Al or Mg–Al hydrotalcite-type materials reveal only broad reflections attributed to impure NiO or MgO crystallites. It has often been hypothesized that the M(III) cations were substituted for M(II) cations in the $M^{II}O$ rock salt-type structures and that their distribution in the $M^{II}O$ crystallites was homogeneous. However, several experimental observations reported previously or in the present work suggest that the homogeneity is questionable and that alumina or aluminate phases might be present in addition to the M(II)O crystallites.

1. It must be underlined that the studied materials are very poorly crystallized. The possibility that X-ray amorphous phases are formed must be taken into account. The reasoning developed on the MgO or NiO patterns is likely to concern only a fraction of studied materials. X-ray diffraction data on sample A calcined between 573 and 1123 K have been previously reported.[25,26] No phase other than NiO was detected. The NiO reflections were shifted toward 2θ values higher than those corresponding to pure NiO, which was attributed to the substitution of Al(III) for Ni(II) cations in the NiO lattice. No additional reflection, such as that visible in the XRD patterns of samples B–D, was observed; however, the (111) reflection is much more intense in nickel oxide than in magnesia, and a weak reflection around $d = 0.253$ nm could be ignored. For samples calcined at temperatures higher than 923 K, the NiO distorsion (lattice parameters shifts, variation of the relative intensities of the reflections) became negligible. Thus, the presence of aluminum containing X-ray amorphous phases in addition to NiO was highly probable.

In calcined samples B–E, a reflection not belonging to the NaCl-type lattice is observed. This reflection is also observed when X-ray diffraction is performed in an *in situ* cell to avoid possible rehydration. It is observed for calcination temperatures higher than required for complete decarbonation or dehydroxylation, i.e., 873 K. Thus, the additional reflection is not due to hydrotalcite. The additional reflection can be attributed either to a magnesium aluminate-type phase or to a sublattice of Al(III) or Mg(II) cations on tetrahedral, interstitial sites in MgO. This finding is consistent with the NMR data revealing tetrahedrally coordinated aluminum, in accord with previous studies.[18,34,36,49] Either the distribution of cations is homogeneous in the magnesia particles, in this case the obtained oxides do *not* have the NaCl-type structure, or another phase, i.e., likely nonstoichiometric magnesium aluminate, is present in addition to MgO. The latter hypothesis is more likely since the additional reflection is much broader than the MgO reflections. In brief, there is some doubt that the mixed oxides are single phase.

2. EXAFS measurements performed on the isomorphous systems $MgO–Ga_2O_3$ have revealed that only a minor fraction of Ga(III) ions substitutes for Mg(II) ions in the magnesia lattice. In other words, gallium-rich phases are present in addition to MgO in calcined sample E. EXAFS analysis of calcined samples B–D at the Al K-edge is unfortunately not possible, since the closeness of the Mg and Al edges does not enable accurate analysis at both edges.

3. XPS measurements were performed on the Ni–Al mixed oxides in a previous study.[48] A steady decrease of the Ni/Al ratio with increasing calcination temperature was observed, suggesting a surface enrichment in aluminum. Examination of the O(1s) level in calcined sample A revealed two components. The former was attributed to surface oxygen associated with NiO and the latter to surface oxygen associated with a spinel-type phase. An XPS study on the Mg–Al mixed oxides is in progress. A surface enrichment in aluminum and the presence of two distinct O(1s) binding energies is also observed.

4. Hydrothermal treatments performed under mild conditions on calcined sample A produce boehmite in the early stages and then Ni–Al hydrotalcite-like structures, until total rehydration is reached. These findings are consistent with the presence of alumina, possibly Ni-doped, at the surface of the mixed oxides. The alumina is first hydrated giving rise to crystallized boehmite formation. A major point is that nickel hydroxide is never observed. The presence of amorphous nickel hydroxide in addition to boehmite is very unlikely since similar mild hydrothermal treatments have been used successfully to prepare well crystallized nickel hydroxide from gelatinous precipitates.[44] Thus, the amount of nickel in the superficial alumina is suggested to be low. The hydrotalcite-type phase formed subsequently to boehmite is attributed to the hydration of another phase, possibly Al-doped NiO or nickel aluminate phase.

Therefore numerous consistent data suggest that the thermal decomposition of Ni–Al, and Mg–Al, Mg–Ga hydrotalcite-like coprecipitates does not lead to single phase products. It is interesting to note the similarities between the three systems. A remark should be made concerning a relation, often found in the literature, between the "memory effect" and the homogeneity of the mixed oxides. Indeed, the Ni–Al mixed oxides also reform hydrotalcite-type structures under more severe hydrothermal conditions, even though under mild treatments boehmite can be observed. The fact that the hydrotalcite reconstitution readily proceeds in the magnesia based systems at ambient temperature and atmospheric pressure does not firmly support the assumption that calcined samples B–D are single phase materials. Magnesia's affinity for water is so high that surface compounds different from brucite or hydrotalcite can hardly be crystallized.

Effect of Alkaline Leaching on Calcined Samples A–D. We attempted to selectively dissolve surface aluminum-rich phases by leaching of the mixed oxides with alkaline solutions. Indeed, NiO and MgO basic oxides are found to be insoluble in alkaline media. Transition aluminas have amphoteric properties and dissolve in strongly basic as well as in acidic media. We used this properties to investigate the surface composition in calcined samples A–D. Anhydrous alkaline solutions were used for leaching magnesium based oxides to avoid hydrotalcite reconstruction. In all cases, large amounts of aluminum were removed, whereas dissolved Mg(II) or Ni(II) concentrations in the leaching solutions were negligible, see Table 4.

Some remarks should be made concerning the leaching experiments. First, the $NiO–Al_2O_3$ and $MgO–Al_2O_3$ mixed oxides prepared in this work are not microporous, see Table 3. Thus, aluminum is not extracted from the bulk such as is the case for microporous zeolites but rather from the surface region of the oxides. For the same reasons, the hydrothermal treatments performed on NiO based samples are quite different from zeolite steaming. Second, reprecipitation of large amounts of nickel or magnesium hydroxide during leaching, hampering subsequent aluminum removal, is excluded. Indeed, in the case of calcined

(48) Beccat, P.; Roussel, J. C.; Clause, O.; Vaccari, A.; Triflro', F. In *Catalysis and Surface Characterization*; Dines, T. J., Rochester, C. H., Thomson, J., Eds; The Royal Society of Chemistry: Cambridge, 1992; pp 32–41.

(49) McKenzie, A. L.; Fishel, C. T.; Davis, R. J. *J. Catal.* **1992**, *138*, 547–561.

sample A, the EXAFS study showed that the amount of nickel not included in NiO crystallites removed by leaching was negligible. Nevertheless, transmission electron microscopy showed contrasted nickel hydroxide particules on the leached oxides. These particles were readily removed upon rinsing with distilled water. The Ni/Al ratios before and after rinsing were found to be identical. This confirms that the amount of reprecipitated nickel is very low. Transmission electron micrographs of samples B–D are unfortunately less instructive since no great contrast difference between magnesium and aluminum compounds is expected. EXAFS studies at the magnesium K-edge were not performed because the closeness of the Mg and Al edges makes it impossible to accurately determine next nearest backscatterers. Thus, the precipitation of some magnesium ethanolate or oxoethanolate compound cannot be excluded. We also performed alkaline leachings on magnesium and nickel aluminate spinels with surface areas around 60 m^2/g. We found that the amount of aluminum passing into solution was about one-third of the observed amount with calcined sample A or C, even though the aluminum content was five times higher. Furthermore, the surface composition of the spinels as determined by XPS was similar to the bulk composition, i.e., two-thirds of the cations underneath surface hydroxyl groups are Al(III) ions. This seems to indicate that aluminum ions homogeneously arranged with magnesium ions are difficult to extract. In short, in calcined sample A as well as calcined samples B–D, leaching is likely to dissolve superficial aluminum-rich phases and to have no or an extremely slow (kinetically) effect on the remaining oxides.

Owing to the multitude of sites and possible chemical environments in the Al-modified nickel and magnesium oxides, it is most likely that ^{27}Al MAS–NMR cannot provide definitive answers regarding the structural composition of the systems. Furthermore, in the case of the nickel based systems, the signals are generally broadened beyond detection by the paramagnetic Ni^{2+} species. Nevertheless, two results concerning the Al-promoted magnesium oxides are noteworthy. First, the chemical shifts observed are in the range of those reported for alkali- or alkaline-earth aluminate-type compounds.[50] Although the spectra presented here resemble those previously reported for γ-alumina,[51] they are shifted downfield, especially for the tetrahedral resonance (77 *versus ca.* 70 ppm for aluminas). This unusual shift cannot be explained by a high QCC or asymmetry factor due to surface strains, since the second-order quadrupolar shift not removed by MAS is negative.[46] On the other hand, the chemical shift of aluminum is sensitive to the nature of the second coordination sphere.[52] We have also observed a resonance at 76 ppm for a synthetic magnesium aluminate sample. Accordingly, the downfield shift can be taken as an indication of Mg as a next nearest neighbor of aluminum in the oxides.

Second, the decrease of the Al^{IV} contribution upon alkaline leaching strongly suggests a surface enrichment in tetrahedral aluminum in the Al-promoted MgO. Taking into account the Al^{IV}/Al^{VI} ratios in calcined sample D before and after leaching and the amount of aluminum removed (approximately 30%, see Table 4), the Al^{IV}/Al^{VI} ratio in the phase which has been dissolved can be easily estimated. A value of 1.0 is found. The site distribution in the Al-promoted MgO before leaching is not homogeneous. Al^{IV} preferentially concentrates in the oxide surface region.

It is interesting to compare the amount of removed Al(III) ions with that required for a monolayer coverage, without making any assumption on the validity of our concept. The principal crystal faces present on NiO and MgO are the (100), (110), and (111) faces, with O^{2-} densities of 1.1×10^{19}, 0.8×10^{19}, and 1.3×10^{19} ions/m^2, respectively.[53] Thus the close-packing monolayer capacity of alumina on NiO and MgO should be lower or equal to 0.9×10^{19} Al(III) ions/m^2. In calcined samples A and D, this leads to Al monolayer capacities of 2.1 and 2.3×10^{-3} mol/g, respectively, using the specific surface areas indicated in Table 3. In calcined sample A (NiO based), the amount of removed aluminum is higher than the monolayer capacity. In calcined sample D, more than half of the monolayer capacity is removed upon leaching. This clearly shows that the impact of the superficial aluminum-rich phases on the surface properties of the mixed oxides (acidity, catalysis, thermal stability) cannot be neglected. An IR investigation using methanol and pyridine as probe molecules to study the adsorption sites of the Al-modified MgO systems is in progress.[54]

Calcined Hydrotalcite-Type Coprecipitates: Compositional Fluctuations. The demixing of calcined hydrotalcite-type materials into well crystallized oxide and spinel phases upon calcination at high temperatures is well-known. When calcined at lower temperatures, hydrotalcite structures form thermally stable oxides for which numerous applications have been considered. However, little is known about the phase composition in these oxides, since the X-ray diffraction patterns show badly crystallized phases. We suggest that XRD only reveals a fraction of the systems and that X-ray amorphous phases play a major role for the thermal stability and surface properties of the studied Al-modified MgO and NiO oxides. In other words, considering calcined hydrotalcites as mixed oxides in which cations are homogeneously distributed would be an oversimplification which might lead to false conclusions concerning the surface composition.

The stable decomposition products of Mg–Al or Ni–Al hydrotalcite-like coprecipitates at high temperature are pure magnesium (or nickel) oxide and magnesium (or nickel) aluminate. Thus, the mixed oxides obtained for intermediate calcination temperatures are nonequilibrium oxide solutions. Actually, hydrotalcites belong to the large class of mixed carbonates and the mechanism of their thermal decomposition strongly resembles that of other mixed carbonates such as, for example, dolomite $CaMg(CO_3)_2$. Upon heating at temperatures lower than required for demixing, the cations and oxide anions do not undergo long-range diffusion but only short-range or local rearrangements, which lead to topotactic transformations. The platelet-type morphology of the coprecipitates is retained in the mixed oxides.[25] The cation distribution in the platelets is, however, not homogeneous. This result is in good agreement with a recent study devoted to the thermal decomposition of dolomite.[23] The chemical decomposition of dolomite was suggested to lead to spinodal solutions, the wavelength of compositional fluctuations from Mg to Ca rich regions being approximately 5 nm. In our case, it is not possible to specify whether the Al-stabilized nickel and magnesium oxide phases are spinodal solutions or interconnected discrete nucleated particles of MgO (or NiO) and spinel phases. Nevertheless, the compositional fluctuations from Mg (or Ni) and Al-rich zones are likely to induce surface compositions different from those dictated by a homogeneous cation distribution in the oxides. This provides an explanation for the abnormally high Al surface concentrations revealed by the leaching experiments. The concept of short-range compositional fluctuations may also apply for other systems obtained by calcination of coprecipitates, mixed carbonates or mixed gels, such as the methanol and alcohol synthesis catalysts. This concept makes it possible to understand how large surface enrichments may occur in systems which seem to be homogeneous at the 10-nm scale.

(50) Müller, D.; Gessner, W.; Samoson, A.; Lippmaa, E.; Scheler, G. *J. Chem. Soc., Dalton Trans.* **1986**, 1277–1281.
(51) Morris, H. D.; Ellis, P. D. *J. Am. Chem. Soc.* **1989**, *111*, 6045–6049.
(52) Müller, D.; Gessner, W.; Behrens, H. J.; Scheler, G. *Chem. Phys. Lett.* **1981**, *79*, 59–62.
(53) Gu, Y. L.; Brenner, A. *J. Catal.* **1992**, *136*, 222–231.
(54) Lavalley, J. C.; Bachelier, J. C.; Lahousse, C.; Clause, O., manuscript in preparation.
(55) Clause, O.; Bonneviot, L.; Che, M.; Dexpert, H. *J. Catal.* **1991**, *130*, 21–28.
(56) Clause, O.; Bonneviot, L.; Che, M. *J. Catal.* **1992**, *138*, 195–205.

The concept of short-range compositional fluctuations gives a macroscopic representation of the mixed oxides. Another way of describing the promotion of MgO or NiO by Al^{3+} ions starts from the $M^{II}O$ phase and specifies the bulk and surface modifications induced by the promoter. This description may be viewed as "microscopic". A three-phase model is proposed to involve the formation of Al-doped NiO or MgO crystallites, Ni- or Mg-doped alumina, and an aluminate spinel-type phase at the $M^{II}O$-alumina interface.

Al-doped NiO or MgO phases are clearly revealed by X-ray diffraction. They form the crystallized fraction of the systems.

Ni- or Mg-doped alumina phases are revealed by alkaline leaching. Broadly speaking, alumina represents about one-third of aluminum in samples B–D and two-thirds in sample A, all calcined at 923 K. The amount of nickel dissolved in alumina is suggested to be low for sample A, since reprecipitated nickel hydroxide can be detected neither by X-ray fluorescence (before and after rinsing with distilled water) nor by EXAFS. In the NiO based systems the alumina phase can be rehydrated to boehmite. The removal of alumina has only a minor effect on the thermal stability of samples A–D, see Figure 11 and ref 25. Likewise, the thermal stability of sample A is not altered significantly by crystallization of boehmite upon mild hydrothermal treatments. Alumina plays a minor role in the thermal properties of the Al-promoted magnesium and nickel oxides.

Nickel or magnesium aluminate phases are suggested to be present in leached samples A–D. XPS studies performed on Ni–Al calcined hydrotalcites revealed a large surface enrichment in aluminum even after alkaline treatment. Likewise, analysis of the O(1s) level in leached sample A revealed a large fraction of surface oxygen associated with a spinel-type phase, possibly nickel aluminate.[48] An XPS study is in progress on calcined samples B–D and similar conclusions can be reached. On the other hand, the XRD additional reflection attributed to a nonstoichiometric magnesium aluminate phase does not disappear upon alkaline leaching, see Figure 11. The nonstoichiometric aluminate lattice is thought to be in strong interaction with that of the underlying NaCl-type oxide. In the case of the Al-doped MgO, the lattice parameter of the aluminate is twice that of magnesium oxide.

Aluminum represents a minor fraction of cations present in samples A–D. A fraction (most certainly large) of the aluminum ions forms alumina and aluminate phases at and on the surface of the MgO (NiO) particles. Thus, the MgO and NiO crystallites can be viewed as decorated by spinel-type phases. This conclusion can most probably be extrapolated to other mixed oxides obtained by calcination of single-phase precursors. For example, the formation of gallium-rich phases upon calcination of Mg–Ga hydrotalcite-like coprecipitates is suggested in this work. A similar conclusion can be reached when iron is substituted for gallium or aluminum. A second example consists of silicates with a layered structure which are formed during the preparation of Ni/SiO_2 systems either by the deposition–precipitation or the "ion exchange" techniques.[44,55] The thermal decomposition of the silicates leads to small nickel oxide crystallites decorated with silica.[56] Consequently, decorated nickel oxide is much more difficult to reduce compared to pure nickel oxide.

Aluminum has a major effect on the thermal stability of magnesium or nickel oxide. It is interesting to correlate this stabilizing effect to the ability of aluminum to reside either on the surface or in lattice sites in Mg(Ni)O. First, we have observed that the alumina phase plays only a minor role on the resistance of NiO or MgO to sintering, see Figures 8 and 11. Alumina removal results in a slight increase of the $M^{II}O$ crystal sizes. In the leached materials, aluminum ions are incorporated in the NiO or MgO lattice, possibly as surface-spinel type compounds, or at least on tetrahedral interstitial sites in the MgO case. This behavior illustrates the effect of incorporation of foreign ions into the $M^{II}O$ lattice versus deposition onto the lattice.

The aluminum ions remaining after alkaline leaching are responsible for the thermal stability of the magnesium or nickel oxide phases. We suggest that the formation, at the surface of the oxides, of nickel or magnesium aluminate-type phases decreases the oxide sintering through reducing interparticle bridging and hindering surface diffusion. Indeed, sintering requires diffusion of both cations and oxide ions. In other words, the thermal behavior is that of the surface spinels.

Conclusions

In this work, the phase composition of Al-modified nickel and magnesium oxides obtained by calcination of homogeneous precursors is investigated by X-ray diffraction, ^{27}Al MAS–NMR, and EXAFS. Some insight into the surface composition is gained employing alkaline leachings. The use of anhydrous alkaline solutions is shown to be of interest for investigating the surface composition of oxides which easily rehydrate, such as magnesia-based systems. Calcination of Ni–Al and Mg–Al hydrotalcite-like compounds gives nonequilibrium oxide solutions, which is reminiscent of the spinodal solutions obtained by thermal decomposition of dolomite. Aluminum-rich phases, likely aluminas and magnesium or nickel aluminates, are detected in the surface region of the Al promoted NiO and MgO systems. The alumina phases are found to play a minor role in the thermal stability of the oxides and can be viewed as deposited onto the $M^{II}O$ and/or aluminate-type phases. On the other hand, nonstoichiometric aluminate-type phases decorating the MgO or NiO crystallites are thought to be responsible for the resistance to thermal sintering of the magnesium or nickel oxide.

Acknowledgment. We express our thanks to E. Ubrich for TGA measurements, to J. C. Roussel for help during NMR measurements, to F. Villain for help during EXAFS measurements, and to Mrs. Retou and Jacoboni (Laboratoire des Fluorures, Université du Maine, Le Mans) for performing *in situ* XRD powder pattern acquisitions. Stimulating discussions with Drs. C. Cameron, C. Marcilly, and Ph. Courty are gratefully acknowledged.